

# 変分マルチスケールに基づく安定化Space-Time有限要素法を用いた堤体の越流崩壊解析

## Variational Multi-scale Stabilized Space-Time Finite Element Method for Simulating Overtopping Failure of Embankment

○ Sharma VIKAS\*, Kazunori FUJISAWA\*

### 1. Introduction

The coupled analysis of the seepage flow in porous media and regular incompressible flow in the fluid domain (henceforth, Navier-Stokes flow) is of paramount importance for the risk assessment of the earthen structures (viz., embankment, levee, canal, etc.) and natural slopes against the erosion, piping, tidal waves, among others. The seepage flow and the Navier-Stokes flow have different flow characteristics; the speed of fluid in porous media is relatively smaller than that in fluid domain. Furthermore, the seepage flow is mainly governed by the frictional forces, whereas, the Navier-Stokes flow is governed by the combined action of the inertia force, viscous force and the pressure gradient. Due to these differences in flow characteristics the simultaneous analysis of coupled flow still remains a challenging task. Therefore, the aim of this study is to develop a finite element method for simultaneous computation of numerical solution of the coupled flow in porous domain and fluid domain.

### 2. Governing equations

Let  $\Omega^f$  and  $\Omega^s$  be the non-overlapping fluid and soil domain, and let  $\Omega := \Omega^f \cup \Omega^s$  be the computation domain. In this study, the Darcy-Brinkman equations (DBE), which are given by Eq. 1 and Eq. 2, are employed to describe the fluid flow in fluid and porous domains in a unified manner. In these equations,  $\rho$  denotes the

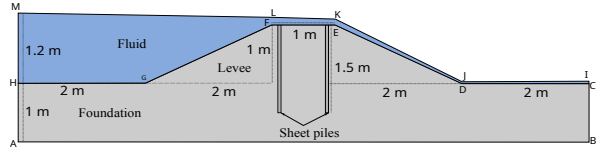


Figure 1: Finite element model of river-levee system

density of fluid,  $\mathbf{v}$  and  $p$  denote the velocity and pressure of the fluid,  $\phi$  is the porosity ( $\phi = 1$  in  $\Omega^f$ ),  $\mu$  is the dynamic viscosity of the fluid,  $K$  is the permeability of the porosity ( $K^{-1} = 0$  in  $\Omega^f$ ),  $\mathbf{g}$  is the acceleration due to gravity, and  $\boldsymbol{\tau}$  is the shear-stress tensor, which is given by  $\boldsymbol{\tau} = \mu(\mathbf{v} \otimes \nabla + \nabla \otimes \mathbf{v})$ .

$$\mathbf{r}_M(\mathbf{v}, p) := \rho \frac{\partial \mathbf{v}}{\partial t} + \rho \left( \frac{\mathbf{v} \otimes \mathbf{v}}{\phi} \right) \cdot \nabla - \boldsymbol{\tau} \cdot \nabla + \frac{\mu \phi}{K} \mathbf{v} + \phi \nabla p - \rho \phi \mathbf{g} = \mathbf{0} \quad (1) \quad r_c(\mathbf{v}) := \nabla \cdot \mathbf{v} = 0 \quad (2)$$

### 3. Variational multi-scale space-time formulation

The main challenges in solving the DBE can be attributed to (a) ensuring the compatibility condition between the pressure and the velocity fields (also known as *Ladyzhenskaya-Babuska-Brezzi* condition), (b) suppressing the numerical instability due to the presence of large convective terms, and (c) handling the deforming spatial domain due to the presence of free-surface and surface erosion of porous media.

Therefore, to overcome these challenges, variational multiscale space-time finite element method (VMS-ST/FEM) is employed. Let  $\mathcal{V}_v$  and  $\mathcal{V}_p$  be the space of trial functional space for velocity and pressure, and  $\delta\mathcal{V}_v$  and  $\delta\mathcal{V}_p$  be the space of test functions for  $\mathbf{v}$  and  $p$ . Then the weak form of VMS-ST/FEM is given by: find  $(\tilde{\mathbf{v}}, \tilde{p}) \in \mathcal{V}_v \times \mathcal{V}_p$ , such that  $\forall (\delta\tilde{\mathbf{v}}, \delta\tilde{p}) \in \delta\mathcal{V}_v \times \delta\mathcal{V}_p$  Eq. (3) is true. In Eq. (3),  $\tilde{\mathbf{v}}$  and  $\tilde{p}$  denote the fine scale components of velocity and pressure field, respectively, and are given by Eq. (5) and Eq. (6), respectively. In these equations,  $\tau_s$  and  $\nu_{lisc}$  are the stabilization parameters.

\*京都大学 農学研究科, Graduate School of Agriculture, Kyoto University

**Keywords:** Space-Time FEM, Multiscale, Darcy-Brinkmann

$$\begin{aligned}
& \left( \delta \bar{\mathbf{v}}, \rho \frac{\partial \bar{\mathbf{v}}}{\partial t} + \left( \frac{\rho \bar{\mathbf{v}} \otimes \bar{\mathbf{v}}}{\phi} \right) \cdot \nabla + \frac{\mu \phi}{K_0} \bar{\mathbf{v}} \right)_{Q_n} + (\delta \bar{\mathbf{v}} \otimes \nabla, \bar{\boldsymbol{\tau}})_{Q_n} - (\nabla \cdot (\phi \delta \bar{\mathbf{v}}), \bar{p})_{Q_n} + (\delta \bar{p}, -\phi \nabla \cdot \bar{\mathbf{v}})_{Q_n} + (\delta \bar{\mathbf{v}}_n, \rho (\bar{\mathbf{v}}_n^+ - \bar{\mathbf{v}}_n^-))_{\Omega_n} \\
& + \sum_e \left( -\delta \bar{\mathbf{v}} \otimes \nabla, \frac{\rho}{\phi} (\bar{\mathbf{v}} \otimes \bar{\mathbf{v}} + \bar{\mathbf{v}} \otimes \bar{\mathbf{v}}) \right)_{Q_e} + \sum_e \left( -\delta \bar{\mathbf{v}} \otimes \nabla, \frac{\rho}{\phi} \bar{\mathbf{v}} \otimes \bar{\mathbf{v}} \right)_{Q_e} + \sum_e (-\nabla \cdot (\phi \delta \bar{\mathbf{v}}), \bar{p})_{Q_e} \\
& + \sum_e \left( -\rho \frac{\partial \delta \bar{\mathbf{v}}}{\partial t} - \nabla \cdot \delta \bar{\boldsymbol{\tau}} + \frac{\mu \phi}{K_0} \delta \bar{\mathbf{v}} + \nabla (\phi \delta \bar{p}), \bar{\mathbf{v}} \right)_{Q_e} - \sum_e (\delta \bar{\mathbf{v}}, \bar{\boldsymbol{\sigma}} \mathbf{n})_{\partial Q_e} - (\delta \bar{\mathbf{v}}, \rho \phi \mathbf{g})_{Q_n} = 0
\end{aligned} \quad (3)$$

$$\tilde{\mathbf{v}} = -\frac{\tau_s}{\rho} \mathbf{rM}(\bar{\mathbf{v}}, \bar{p}) \quad (4)$$

$$\tilde{p} = -\rho \nu_{sic} r_c(\bar{\mathbf{v}}) \quad (5)$$

$$\frac{1}{\tau_s} = \frac{1}{|\tau_{12}|} + \frac{1}{|\tau_3|} + \frac{1}{|\tau_4|} \quad (6)$$

$$\frac{1}{\tau_{12}} = \sum_{a=1}^{n_{nt}} \sum_{l=1}^{n_{ns}} \left| \frac{\partial N^l T_a}{\partial t} + \bar{\mathbf{v}} \cdot \nabla (N^l T_a) \right| \quad (7)$$

$$\frac{1}{\tau_3} = \frac{4\nu}{h_{RCN}^2} \quad (8) \quad \frac{1}{\tau_4} = \frac{2\mu\phi}{\rho K} \quad (9)$$

$$\nu_{sic} = \begin{cases} \frac{h_{RCN}^2}{\tau_s} & \text{in } \Omega^f \\ \frac{h_{RCN} L_0}{\tau_s} & \text{in } \Omega^s \end{cases} \quad (10)$$

$$\frac{1}{h_{RCN}} = \frac{1}{2} \sum_{a=1}^{n_{nt}} \sum_{l=1}^{n_{ns}} \left| \frac{\nabla \|\tilde{\mathbf{v}}\|}{\|\nabla \|\tilde{\mathbf{v}}\|} \cdot \nabla (N^l T_a) \right| \quad (11)$$

In Eq. (10),  $L_0$  denotes the characteristic length, in Eq. (11),  $\|\cdot\|$  denotes the  $L_2$  norm,  $n_{nt}$  and  $n_{ns}$  denote the number of temporal and spatial nodes in a space-time element, and  $N^l T_a$  denotes the shape function at  $l$ th spatial and  $a$ th temporal node of space-time element.

#### 4. Results and discussions

Figure 1 depicts the finite element model of river-levee system, in which the levee is equipped with a dual sheet-pile system for its strengthening against the overtopping failure. In this study, the value of  $\phi$  for soil (both levee and foundation), sheet-pile, and water is 0.5, 0.01 and 1.0, respectively. The permeability of soil, sheet-pile and water is  $10^{-10} \text{ m}^2$ ,  $10^{-30} \text{ m}^2$ , and  $10^{30} \text{ m}^2$ , respectively. The viscosity of water is 0.001 Pa.s. The initial profile of water, that is, height of segments CI (0.04 m), DJ (0.03 m), EK (0.1 m), FL (0.13 m) as shown in Figure 1 is obtained by solving the shallow water equation. The initial condition for  $\mathbf{v}$  and  $p$  corresponds to the hydrostatic conditions. On the boundary HM,  $\mathbf{v} = (0.083, 0) \text{ m/s}$ , whereas on the boundary AH,  $\mathbf{v} = 0$  is prescribed. The boundary IJKLM is a free-surface where  $p = \rho g y$  is prescribed as Neumann boundary condition. On the outlet boundary CI  $p = \rho g y$  is prescribed, and on the boundary BC  $p = 0$  is prescribed. On the boundary AB  $v_y = 0$  is prescribed as the Dirichlet boundary condition. The computation domain changes due to the movement of free-surface. The present study employs an elasticity based mesh moving scheme (see, [1] for more details). After achieving the near steady-state, the downstream slope of levee (segment CDE) is allowed to erode due to the surface flow. The rate of erosion is given by following equation:

$$E_r = \begin{cases} \alpha_e \left( \frac{v_b^2}{v_{bc}^2} - 1 \right)^{\gamma_e} & v_b \geq v_{bc} \\ 0 & v_b < v_{bc} \end{cases}$$

where,  $\alpha_e = 5.33 \times 10^{-4} \text{ m/s}$ ,  $v_{bc} = 0.2 \text{ m/s}$ , and  $\gamma_e = 1.5$  are erosion parameters, and  $v_b$  is the tangential velocity near the soil-water interface. The results of deformed configuration (after erosion), pressure and velocity distribution are shown in Figure 2 which demonstrate that VMS-ST/FEM with moving mesh technique provides an efficient strategy for simulating the erosion processes in earthen dams.

#### References:

[1] Sharma, V., Fujisawa, K., & Murakami, A. (2021). Space-time finite element method for transient and unconfined seepage flow analysis. *Finite Elements in Analysis and Design*, 197, 103632.

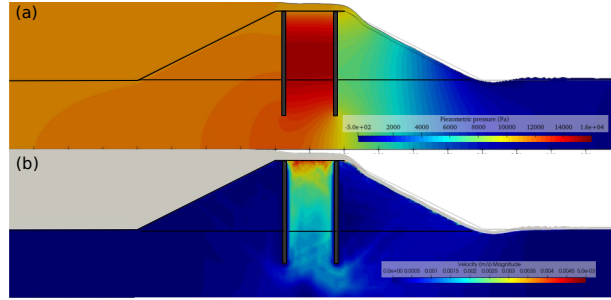


Figure 2: (a) Piezometric pressure field in the river-levee system, and (b) velocity field in the soil